



# CuAAC click chemistry for the enhanced detection of novel alkyne-based natural product toxins†

Cite this: *Chem. Commun.*, 2018, **54**, 12234

Received 20th July 2018,  
Accepted 17th September 2018

DOI: 10.1039/c8cc05113e

rsc.li/chemcomm

Edward S. Hems,  ‡ Ben A. Wagstaff, ‡ Gerhard Saalbach and Robert A. Field  \*

**In the context of discovering and quantifying terminal alkyne-based natural products, here we report the combination of CuAAC click chemistry with LC-MS for the detection of polyether toxins (pymnesins) associated with harmful algal blooms. The added-value of the CuAAC-based approach is evident from our ability to detect novel pymnesin-like compounds in algal species with previously uncharacterised toxins.**

*Prymnesium parvum* is a toxin-producing microalga that causes harmful algal blooms globally, frequently leading to large-scale fish kills that damage ecosystems and the economy of the affected areas.<sup>1</sup> We recently reported upon our efforts to tackle blooms of this microalga on the Norfolk Broads in the East of England.<sup>2–4</sup> Although several toxic compounds have been reported from *P. parvum*,<sup>5–7</sup> the toxins responsible for fish kills are believed to be the ichthyotoxic pymnesins—potent ladder-frame polyethers decorated with uncommon structural features, such as chlorine and alkynes (Fig. 1). First discovered and structurally characterized in 1996,<sup>8,9</sup> the pymnesins were only relatively recently detected by other research groups,<sup>10,11</sup> who have suggested that a challenge may lie in the chemodiversity of this class of toxins.<sup>11</sup> Initially aiming to employ CuAAC derivatization of the terminal alkyne group present in pymnesins for their facile fluorescence detection, herein we illustrate how this chemistry is invaluable for enhancing LC-MS-based detection of new alkyne-based natural product toxins.

Current classification of the pymnesins groups them into either A-, B- or C-type based on their polyether core, sub-divided by the extent of chlorination and the nature and extent of their glycosylation (Fig. 1).<sup>11</sup> Detection of pymnesins typically relies upon LC-MS analysis<sup>10,11</sup> or labelling of the conserved amine group with ninhydrin and phenylacetaldehyde to give a

fluorescent adduct.<sup>12</sup> We were drawn to consider whether the conserved terminal bis-alkyne on pymnesin toxins might prove to be a useful chemical handle for the detection of pymnesins via the ubiquitous bioorthogonal copper-catalysed alkyne-azide cycloaddition (CuAAC) ‘click’ reaction, which has been deployed in a number of diagnostic contexts.<sup>13</sup> The detection of a terminal alkyne-based plant natural product using this approach was reported recently.<sup>14</sup> Terminal bis-alkynes, as in the pymnesins, are rare moieties in nature, with interesting chemical and spectroscopic properties.<sup>15,16</sup> We were therefore minded to explore the possibility of specifically labelling pymnesins through CuAAC click chemistry to aid their detection and characterisation. Since it is challenging to obtain quantities of pymnesins from laboratory scale cultures,<sup>8,11</sup> preliminary experiments required synthetic terminal alkyne (1) and bis-alkyne (2), which were prepared as set out in Scheme S1 (ESI†). In trial reactions with 3-azido-7-hydroxycoumarin (3),<sup>17,18</sup> CuAAC reaction efficiencies for alkyne 1 and bis-alkyne 2 were broadly similar (Fig. S1, ESI†), showing that terminal bis-alkynes are indeed good candidates for targeted CuAAC click chemistry (Fig. 2).

Next, we investigated whether CuAAC click chemistry could be utilised to detect pymnesin toxins from laboratory cultures of *Prymnesium* (Table S1, ESI†). Previous work<sup>10,11</sup> has shown that pymnesins display diagnostic isotope patterns in MS data, in part related to the number of chlorine atoms present. Furthermore, pymnesins fly as double-charged ions, fragmenting readily to the aglycone form of the toxin, which is often the most abundant ion present. We first sought to use CuAAC click chemistry to detect pymnesins from *P. parvum* (946/6), a strain which is known to produce the ‘A-type’ pymnesins-1 and -2 (referred to as pymnesin-A1 and -A2 hereafter).<sup>19</sup> Pymnesin toxins were extracted from lab grown cultures of *Prymnesium* using a modification of published procedures<sup>10</sup> and subjected to LC-MS analysis. Using this approach, we could identify signals for previously characterized pymnesin-A1 and -A2 from *P. parvum* 946/6 (Fig. 3 and Fig. S3, ESI†), which we also later detected in the *P. parvum* 94A strain (Fig. S4, ESI†). The extracts containing the ‘A-type’ pymnesins were subjected to CuAAC

Department of Biological Chemistry, John Innes Centre, Norwich Research Park, Norwich, NR4 7UH, UK. E-mail: rob.field@jic.ac.uk

† Electronic supplementary information (ESI) available. See DOI: 10.1039/c8cc05113e

‡ Edward S. Hems and Ben A. Wagstaff contributed equally to this study.



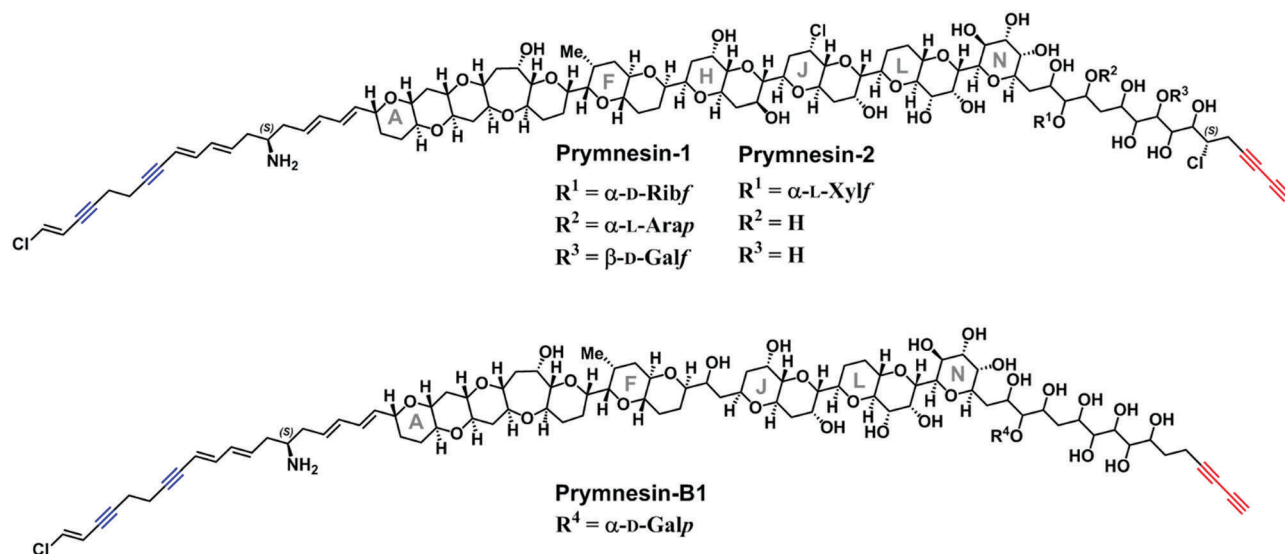


Fig. 1 The reported structures of the known pymnesin toxins.<sup>8,9,11</sup> Blue = internal alkynes. Red = terminal bis-alkyne. Note that despite the variation between pymnesin-1/2 and pymnesin-B1 toxins, the number and relative locations of the alkynes are conserved.

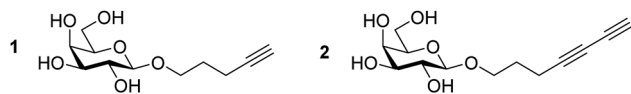


Fig. 2 Target mono- (1) and bis-alkyne (2) pymnesin model compounds produced synthetically as set out in Scheme S1 (ESI†).

click chemistry with **3** under similar conditions to those described for model alkynes **1** and **2**. If the click reaction was successful, we would expect the formation of new pymnesin-like molecules coupled to the coumarin chromophore *via* a triazole ring. Before re-examining these clicked extracts using LC-MS, they were subjected to TLC analysis,<sup>10</sup> which confirmed the formation of new products visible by long wave UV (365 nm) (Fig. S2, ESI†). In future, this TLC analysis may be exploited as a tool to simply assess the presence of toxins of this type in other algal strains or even natural water samples.

Next, the clicked extracts were examined by LC-MS to see if masses corresponding to the 'clicked' pymnesin-A1 and -A2 toxins could be identified. Signals previously assigned as originating from these toxins were found to increase in mass by the expected value of  $m/z \sim 101.5$  for the addition of 3-azido-7-hydroxycoumarin (**3**) (Fig. 3A). For pymnesin-A1 and -A2, which share the same backbone mass (aglycone) of  $\sim 918.9$  ( $m/z$  ion), this click conjugation with **3** was reflected by an increase in mass of  $\sim 101.5$  to  $\sim 1020.4$  (Fig. 3C). The reaction with **3** did not affect the fragmentation pattern of the toxins, with pymnesin-A1 showing  $m/z$  losses of 66 and 81, corresponding to losses of 2 pentose units and 1 hexose from the intact form of the toxin (Fig. 3C). Pymnesin-A2 is only glycosylated at a single position with a pentose, and subsequently shows only 1 fragmentation loss of  $m/z$  66 corresponding to the loss of this pentose. Measured isotope distribution patterns for both the non-clicked and clicked toxins match theoretical predictions calculated using enviPat<sup>20</sup> (Fig. S7 and S8, ESI†).

Using this methodology, we next identified pymnesin-like compounds from the *P. sp.* 595 strain with a similar backbone composition to those of the previously reported 'B-type' toxins,<sup>11</sup> which we have termed pymnesin-B6 and -B7 (Fig. S5, ESI†). We also detected signals from this strain for pymnesin-B1 and the non-glycosylated form of pymnesin-B1, but at much lower intensities (Table S2, ESI†). Pymnesin-B6 and -B7 show increased levels of chlorination compared to pymnesin-B and -B1,<sup>11</sup> which is reflected by the corresponding double charged ions of the backbone of pymnesin-B6 and -B7 being  $m/z$  17 units higher. Pymnesin-B6 shows no obvious fragmentation, and we therefore speculate this compound is not glycosylated. Pymnesin-B7 shares the same backbone as B6 but shows a single fragmentation loss of  $m/z$  81, corresponding to the loss of a hexose. Upon CuAAC click coupling of these putative toxins with azido-coumarin **3**, both show increases in their backbone masses from  $\sim 845.9$  by  $\sim 101.5$  units to  $\sim 947.4$ , suggesting that these compounds also share the terminal alkyne system observed in all pymnesins reported to date. As with pymnesin-A1 and -A2, click coupling to **3** did not alter fragmentation patterns and measured isotope distribution patterns match theory (Fig. S9, ESI†). Due to the much lower intensities of pymnesin-B and -B1 in the extracts, signals corresponding to the clicked products of these toxins could not be observed.

We could find no evidence for the previously reported 'C-type' pymnesins<sup>11</sup> in any of the 4 strains that we examined. However, in *P. patelliferum* 527D, we detected signals for novel alkyne-containing molecules with distinct backbone masses and elemental compositions. The nature of the toxin produced by this *Pymnesium* genus has yet to be confirmed.<sup>21</sup> We termed these compounds pymnesin-D1 to -D4, and suggest that they make up a new 'D-type' family of pymnesin toxins, based on positive CuAAC derivatization (Fig. 4). Pymnesin-D1 and -D2 share a  $m/z$  backbone mass of  $\sim 883.8$  and are glycosylated in a similar manner to pymnesin-A1 and -A2: D1 shows fragmentation



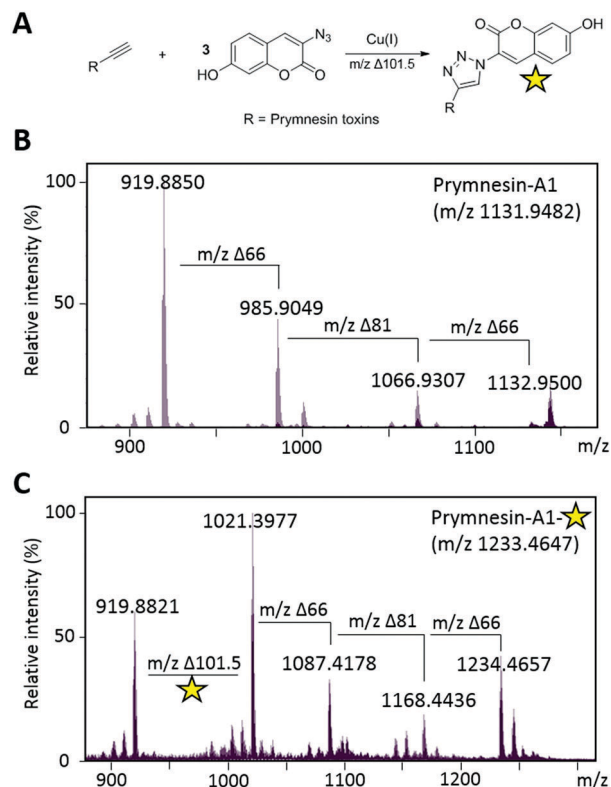


**Fig. 3** Click coupling of prymnesin-A1 from *P. parvum* 946/6 culture extracts. (A) Reaction scheme for the CuAAC click coupling of 3-azido-7-hydroxycoumarin (**3**) with prymnesin toxins. Yellow star represents the activated fluorescent triazole product. (B) MS/HRMS spectra of  $[M + 2H]^{2+}$  for previously reported prymnesin-A1.  $\Delta 66$  reflects a loss of a pentose unit and  $\Delta 81$  reflects a loss of a hexose unit. Prymnesin-A1 is triply glycosylated with 2 $\times$  pentose units and 1 $\times$  hexose. (C) MS/HRMS spectra of  $[M + 2H]^{2+}$  for prymnesin-A1 after CuAAC click coupling with **3**.  $\Delta 101.5$  reflects addition of the coumarin moiety to the prymnesin toxin. Fragmentation of pentose and hexose units is still visible after addition of **3**.

loss of 2 pentose units and 1 hexose from the intact compound (Fig. 4), whilst -D2 shows a single fragmentation loss of 1 pentose. Prymnesin-D3 and -D4, respectively, share these glycosylation patterns, but have backbone masses  $m/2$  18 units lower, corresponding to the absence of HCl (Table 1). This lack of HCl suggests the presence of an additional alkene or alkyne moiety, with loss of chlorine, in the toxin backbone. As we do not observe multiple additions of **3** to these toxins, we speculate that the absence of HCl results in a new internal alkene at the glycosylated 'tail' of the toxins or in the polyether ring system (Fig. 1). These D-type toxins display similar levels of unsaturation to the A-type prymnesins, suggesting more alkenes or conjugated ring systems are present in these toxins than in the B and C-type (Table S1, ESI<sup>†</sup>).

Successful CuAAC 'click' coupling of these novel D-type prymnesin-like-compounds confirmed the presence of a single terminal alkyne system, as we also observe mass shifts corresponding to the addition of **3** to these compounds. For prymnesin-D1 and -D2, the double charged backbone mass of  $\sim 883.8$  increases by  $\sim 101.5$  units to  $\sim 985.3$  (Fig. 4B), whilst for prymnesin-D3 and -D4, the double charged backbone mass

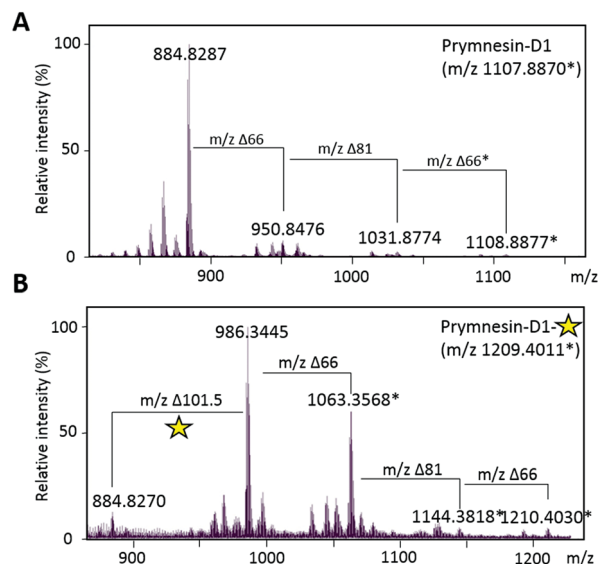


**Fig. 4** Click coupling of putative novel prymnesin-D1 from *P. patelliferum* 527D culture extracts. (A) MS/HRMS spectra of  $[M + 2H]^{2+}$  for prymnesin-D1.  $\Delta 66$  reflects a loss of a pentose unit and  $\Delta 81$  reflects a loss of a hexose unit. Prymnesin-D1 is triply glycosylated with 2 $\times$  pentose units and 1 $\times$  hexose. '\*' represents the  $[M + Na + H]^{2+}$  ion. (B) MS/HRMS spectra of  $[M + 2H]^{2+}$  for prymnesin-D1 after CuAAC click coupling with **3**.  $\Delta 101.5$  reflects addition of the coumarin moiety to the prymnesin toxin. Fragmentation of pentose and hexose units is still visible after addition of **3**. Yellow star represents the activated fluorescent triazole product. '\*' represents the  $[M + Na + H]^{2+}$  ion.

of  $\sim 865.8$  increases by  $\sim 101.5$  units to  $\sim 967.3$  (Table S2 and Fig. S6, ESI<sup>†</sup>). In each case, fragmentation patterns still show the loss of monosaccharides from the intact compounds, while measured isotope patterns match theory well (Fig. S10, ESI<sup>†</sup>). A summary of the major prymnesins found in this study, along with their corresponding masses, can be seen in Table 1.

The discovery of prymnesin-A1 and -A2 from 2 out of 4 strains examined extends the findings of Rasmussen *et al.*,<sup>11</sup> who only found these particular toxins in 1/10 strains that they examined (*i.e.* UTEX-2797), suggesting that these toxins are more widespread than previously thought. In addition, the C-type prymnesins were found in 5/10 strains examined by Rasmussen *et al.*,<sup>11</sup> where we did not find them in any of the 4 strains in this study. Instead, the discovery of a new type of prymnesin-like toxin from *P. patelliferum* 527D, the D-type, shows that more species and strains of *Prymnesium* need to be studied to obtain a more complete picture of the global abundance and chemodiversity of these toxins. Interestingly, Rasmussen *et al.*<sup>11</sup> hinted at a regionality to the toxin types (*i.e.* they found mostly B-type from strains originally isolated from Scandinavia). Our results broadly agree with this suggestion, with an A-type producer originally isolated from North America (*P. parvum* 94A), and the B-type producer originally isolated off the coast of Finland (*P. sp.* 595). A summary of the strains used in this study, their place of isolation, and the type of prymnesins that they produce, along with the previous findings of Rasmussen *et al.*,<sup>11</sup> can be found in ESI<sup>†</sup>, Table S1.

Overall, the current study adds a putative new type of prymnesins to the A, B and C-types previously reported.<sup>8–11</sup>



**Table 1** *Prymnesium* strains and corresponding HRMS identification of 8 prymnesin compounds, including prymnesin-A1 and -A2 originally reported by Igarashi *et al.*,<sup>8,9</sup> based on MS/HRMS and subsequent labelling with 3-azido-7-hydroxycoumarin (**3**). Masses reported correspond to  $[M + 2H]^{2+}$  ion, unless denoted with a '\*' which reports the  $[M + Na + H]^{2+}$  ion. Toxins that share the same backbone only have 1 value reported for the clicked aglycone, which is an average signal for the aglycone from all toxins

Strain	Prymnesin-type	Elemental composition of aglycone	$[M\text{-glycone} + 2H]^{2+}$	Elemental composition	$[M + 2H]^{2+}$ $[M + Na + H]^{2+*}$	Elemental composition of 'clicked' toxin (aglycone)	$[M\text{-glycone} + \text{azidocoumarin} + 2H]^{2+}$
<i>P. parvum</i> 946/6	Prymnesin-A1	C <sub>91</sub> H <sub>128</sub> Cl <sub>3</sub> NO <sub>31</sub> (Δ0.6 ppm)	918.8835	C <sub>107</sub> H <sub>154</sub> CUNO <sub>44</sub> (Δ4.0 ppm)	1131.9482	C <sub>100</sub> H <sub>133</sub> CUN <sub>4</sub> O <sub>34</sub> (Δ4.0 ppm)	1020.3965
	Prymnesin-A2	C <sub>91</sub> H <sub>128</sub> Cl <sub>3</sub> NO <sub>31</sub> (Δ1.3 ppm)	918.8853	C <sub>96</sub> H <sub>136</sub> Cl <sub>3</sub> NO <sub>35</sub> (Δ1.5 ppm)	984.9037		
<i>P. parvum</i> 94A	Prymnesin-A1	C <sub>91</sub> H <sub>128</sub> Cl <sub>3</sub> NO <sub>31</sub> (Δ4.6 ppm)	918.8798	C <sub>107</sub> H <sub>154</sub> CUNO <sub>44</sub> (Δ6.0 ppm)	1131.9460	C <sub>100</sub> H <sub>133</sub> Cl <sub>3</sub> N <sub>4</sub> O <sub>34</sub> (Δ6.4 ppm)	1020.3941
	Prymnesin-A2	C <sub>91</sub> H <sub>128</sub> Cl <sub>3</sub> NO <sub>31</sub> (Δ4.2 ppm)	918.8802	C <sub>96</sub> H <sub>136</sub> Cl <sub>3</sub> NO <sub>35</sub> (Δ5.5 ppm)	984.8998		
<i>P. sp.</i> 595	Prymnesin-B6	C <sub>85</sub> H <sub>121</sub> Cl <sub>2</sub> NO <sub>29</sub> (Δ2.1 ppm)	845.8756	C <sub>85</sub> H <sub>121</sub> Cl <sub>2</sub> NO <sub>29</sub> (Δ2.1 ppm)	845.8756	C <sub>94</sub> H <sub>126</sub> Cl <sub>2</sub> N <sub>4</sub> O <sub>32</sub> (Δ5.8 ppm)	947.3884
	Prymnesin-B7	C <sub>85</sub> HmCl <sub>2</sub> NO <sub>29</sub> (Δ3.4 ppm)	845.8745	C <sub>91</sub> H <sub>131</sub> Cl <sub>2</sub> NO <sub>34</sub> (Δ4.9 ppm)	926.8992		
<i>P. patelliferum</i> 527D	Prymnesin-D1	C <sub>85</sub> H <sub>114</sub> Cl <sub>3</sub> NO <sub>32</sub> (Δ0.3 ppm)	883.8270	C <sub>101</sub> H <sub>140</sub> CUNO <sub>45</sub> (Δ0.5 ppm)	1107.8870*	C <sub>94</sub> H <sub>119</sub> Cl <sub>3</sub> N <sub>4</sub> O <sub>35</sub> (Δ0.4 ppm)	985.3437
	Prymnesin-D2	C <sub>85</sub> H <sub>114</sub> Cl <sub>3</sub> NO <sub>32</sub> (Δ3.4 ppm)	883.8298	C <sub>90</sub> H <sub>122</sub> Cl <sub>3</sub> NO <sub>36</sub> (Δ0.5 ppm)	949.8484		
	Prymnesin-D3	C <sub>85</sub> H <sub>113</sub> Cl <sub>2</sub> NO <sub>32</sub> (Δ0.2 ppm)	865.8386	C <sub>101</sub> H <sub>139</sub> ChNO <sub>45</sub> (Δ0.7 ppm)	1078.9063	C <sub>94</sub> H <sub>118</sub> G <sub>2</sub> N <sub>4</sub> O <sub>35</sub> (Δ4.1 ppm)	967.3510
	Prymnesin-D4	C <sub>85</sub> H <sub>113</sub> Cl <sub>2</sub> NO <sub>32</sub> (Δ0.4 ppm)	865.8388	C <sub>90</sub> H <sub>121</sub> Cl <sub>2</sub> NO <sub>36</sub> (Δ0.7 ppm)	931.8589		

Being only the second study to report on novel prymnesin structures, we expect that many more variants are yet to be discovered, as has been seen for the growing number of algal polyether toxins over the last 2 decades.<sup>22</sup> This study also shows the added value of CuAAC click derivatization, in parallel with LCMS analysis, in aiding the detection and discovery of terminal alkyne-containing natural products that are otherwise difficult to identify.

## Conflicts of interest

There are no conflicts to declare.

## Notes and references

- S. R. Manning and J. W. La Claire, *Mar. Drugs*, 2010, **8**, 678–704.
- B. A. Wagstaff, E. S. Hems, M. Rejzek, J. Pratscher, E. Brooks, S. Kuhaudomlarp, E. C. O'Neill, M. I. Donaldson, S. Lane, J. Currie, A. M. Hindes, G. Malin, J. C. Murrell and R. A. Field, *Biochem. Soc. Trans.*, 2018, **46**, 413–421.
- B. A. Wagstaff, I. C. Vladu, J. E. Barclay, D. C. Schroeder, G. Malin and R. A. Field, *Viruses*, 2017, **9**, 40–51.
- E. S. Hems, S. A. Nepogodiev, M. Rejzek and R. A. Field, *Carbohydr. Res.*, 2018, **463**, 14–23.
- H. Kozakai, Y. Oshima and T. Yasumoto, *Agric. Biol. Chem.*, 1982, **46**, 233–236.
- M. J. Bertin, P. V. Zimba, K. R. Beauchesne, K. M. Huncik and P. D. R. Moeller, *Harmful Algae*, 2012, **20**, 117–125.
- J. C. Henrikson, M. S. Gharfeh, A. C. Easton, J. D. Easton, K. L. Glenn, M. Shadfan, S. L. Mooberry, K. D. Hambright and R. H. Cichewicz, *Toxicon*, 2010, **55**, 1396–1404.
- T. Igarashi, M. Satake and T. Yasumoto, *J. Am. Chem. Soc.*, 1996, **118**, 479–480.
- T. Igarashi, M. Satake and T. Yasumoto, *J. Am. Chem. Soc.*, 1999, **121**, 8499–8511.
- S. R. Manning and J. W. La Claire, *Anal. Biochem.*, 2013, **442**, 189–195.
- S. A. Rasmussen, S. Meier, N. G. Andersen, H. E. Blossom, J. O. Duus, K. F. Nielsen, P. J. Hansen and T. O. Larsen, *J. Nat. Prod.*, 2016, **79**, 2250–2256.
- J. W. La Claire, S. R. Manning and A. E. Talarski, *Toxicon*, 2015, **102**, 74–80.
- X. P. He, Y. L. Zeng, Y. Zang, J. Li, R. A. Field and G. R. Chen, *Carbohydr. Res.*, 2016, **429**, 1–22.
- H. Jeon, C. Lim, J. M. Lee and S. Kim, *Chem. Sci.*, 2015, **6**, 2806–2811.
- F. Pertici and R. J. Pieters, *Chem. Commun.*, 2012, **48**, 4008.
- A. L. Shi Shun and R. R. Tykwinski, *Angew. Chem., Int. Ed.*, 2006, **45**, 1034–1057.
- K. Sivakumar, F. Xie, B. M. Cash, S. Long, H. N. Barnhill and Q. Wang, *Org. Lett.*, 2004, **6**, 4603–4606.
- I. M. Ivanova, S. A. Nepogodiev, G. Saalbach, E. C. O'Neill, M. D. Urbaniak, M. A. J. Ferguson, S. S. Gurucha, G. S. Besra and R. A. Field, *Carbohydr. Res.*, 2017, **438**, 26–38.
- B. A. Wagstaff, Doctoral thesis, University of East Anglia, 2017, the Ecology and Glycobiology of *Prymnesium parvum*.
- M. Loos, C. Gerber, F. Corona, J. Hollender and H. Singer, *Anal. Chem.*, 2015, **87**, 5738–5744.
- A. Larsen, W. Eikrem and E. Paasche, *Can. J. Bot.*, 1993, **71**, 1357–1362.
- S. M. Watkins, A. Reich, L. E. Fleming and R. Hammond, *Mar. Drugs*, 2008, **6**, 431–455.

